SPECTRAL AND SPATIAL VARIATIONS OF FLARE HARD X-RAY FOOTPOINTS

L. FLETCHER[1] and H. S. HUDSON[2]
[1]*Department of Physics and Astronomy, University of Glasgow, Glasgow G12 8QQ, U.K.*
(e-mail: lyndsay@astro.gla.ac.uk)
[2]*Space Sciences Laboratory, University of California, Berkeley CA 94720-7450, U.S.A.*
(e-mail: hhudson@ssl.berkeley.edu)

(Received 6 August 2002; accepted 31 August 2002)

Abstract. In a sample of strong RHESSI M-class flares we have made a study of the relationship between the 'hardness' of the HXR spectrum and the intensity in the 30–50 keV energy range. In all events we find clear evidence for a 'soft–hard–soft' pattern of correlation between hardness and flux, on time scales as short as 10 s. We investigate whether or not this pattern is intrinsic to the acceleration mechanism. The RHESSI images in this energy range are dominated by footpoint brightenings, and we have searched for a correlation between footpoint separation velocity and spectral hardness, to be compared qualitatively with theoretical flare models. We find quite systematic footpoint motions, and also note that episodes in which footpoint separation varies rapidly often correspond with episodes of significant change in the flare spectral index, though not as the simplest flare models would predict. We report also on one of our events, on 14 March 2002, which exhibits highly sheared HXR footpoint ribbons extending over a scale of 100 arc sec. For this flare we find a correlation between footpoint motion and hard X-ray flux.

1. Introduction

The hard X-ray (HXR) emission of a solar flare results mainly from the bremsstrahlung of mildly relativistic electrons accelerated in its impulsive phase. This represents the interval of most intense energy release in a flare, often associated with the time of rapid acceleration of an associated coronal mass ejection and launching of a coronal blast wave. In general, accelerated particles carry a large fraction of the magnetic energy released during the impulsive phase, which itself may dominate the total energy of the flare. However, the mechanism and site of impulsive-phase electron acceleration remain unknown. Because the flare energy resides in the coronal magnetic field prior to its release, the site of particle acceleration is presumably also to be found there. However, the bulk of the hard X-radiation (which marks the location of the collisional energy losses of the energetic electrons) normally occurs in the chromospheric footpoints of the coronal loops. These footpoint regions map magnetically to the coronal regions in which the stored magnetic energy becomes converted into kinetic energy of the accelerated particles.

Solar Physics **210:** 307–321, 2002.

With the launching of the Ramaty High-Energy Solar Spectroscopic Imager mission (RHESSI) we have new capability for a systematic exploration, both spectroscopic and imaging, of the flare hard X-ray emissions (Lin *et al.*, 2002). Past observations, almost entirely made with scintillation-counter spectrometers, have typically had energy resolution no better than a few keV in the 10–100 keV energy range; RHESSI uses Ge detectors with resolution on the order of 1 keV and an energy range extending down to a few keV (Lin *et al.*, 2002). The RHESSI imaging throughout this spectral range also provides better sensitivity, dynamic range, and angular resolution than that of the *Yohkoh* Hard X-ray Telescope (HXT; see Kosugi *et al.*, 1991) which has provided the bulk of our current knowledge base in this area.

In this paper we make a first exploration, using RHESSI's new capabilities, of spatial and spectral correlations in the impulsive-phase hard X-ray emission. We choose a sample of strong GOES events and examine the variation of the spectral hardness with (a) HXR intensity and (b) rate of HXR footpoint separation. Past observations have established a 'soft–hard–soft' spectral behaviour throughout flare bursts (Parks and Winckler, 1969; see also Benz, 1977, and the example in Figure 6 of Dennis, 1985). As the burst intensity increases, the photon spectrum hardens, and then softens as the intensity decreases again. This suggests a direct correlation of the flux of accelerated electrons and the 'hardness' of their spectral distribution. These parameters may also be correlated with the rate of separation of flare HXR footpoints, as explained below.

In the reconnection interpretation, the power available for the flare depends on the rate of coronal reconnection. Any reconnection geometry involves the formation of at least one current sheet located at a magnetic separator. Magnetic flux from one magnetic domain reconnects into another domain through this current sheet. The potential drop, V, along a reconnecting current sheet is related to the rate at which magnetic flux reconnects through that sheet:

$$V = \frac{\partial A}{\partial t} = \int E_c \, \mathrm{d}l = \frac{\partial}{\partial t}\left(\int B_\perp \, \mathrm{d}a \right)$$

(e.g., Forbes and Lin, 2000; Qiu *et al.*, 2002). Here E_c is the reconnecting electric field in the corona, l is distance measured along the current sheet, A is the magnetic flux, $B_\perp$ is the normal component of the magnetic field and da is the element of area 'swept out' by the locus of chromospheric points mapping to the reconnecting coronal field. In the simplest symmetric and translationally invariant flare arcade, in which $B_\perp$ remains constant during the flare, the reconnection rate, and the reconnection electric field strength are reflected in the speed $\dot{x}$ at which the locus of footpoints moves. By writing $\mathrm{d}a = L \, \mathrm{d}x$ where L is the current-sheet length, it is found that the electric field strength $E_\circ$ along the X-line above the arcade is given by (e.g., Priest and Forbes, 2002)

$$E_0 = B_\perp(x) \, \dot{x},$$

where x denotes the location of the footpoint.

The events which we examine are clearly not two-dimensional, however the product $B_{\perp}(x) \cdot \dot{x}$ should generally give a measure of the coronal reconnection rate, and hence the power available to accelerate particles. In the simplest interpretation therefore we expect that the peak fluxes, and the highest energy photons, will occur during times of maximum footpoint separation speeds. Clearly there are many model dependences. The flux depends also on the number of particles available to be accelerated which need not depend on the acceleration rate. The geometry of the current sheet, or current sheet turbulence, or the generation of streaming instabilities, could add extra (possibly stochastic) electric field components which act collectively on the distribution of particles to be accelerated.

Recent work from several groups aims at relating the properties of the accelerated particles with footpoint motion or flare ribbon development. Sakao, Kosugi, and Masuda (1998) using *Yohkoh* HXT present the footpoint separation in a single event, finding an overall increase in separation over 30 s of the flare impulsive phase, with superposed small increases and decreases. This event showed no clear time correlation between the burst intensity and the separation rate. However, over a sample of 14 flares it was found that those exhibiting positive separation speeds tended to show upward-breaking HXR spectra, rather than the downward breaks of those events exhibiting zero or negative separation speeds. Qiu *et al.* (2002) look in detail at the motion of the brightest pixels of Hα flare footpoints (marking the sites of chromospheric excitation by electron beams) in a flare observed by Big Bear Solar Observatory and *Yohkoh* HXT. Two almost stationary kernels and two Hα flare 'ribbons' were present in the event, however these were found to remain more or less fixed in position. Systematic kernel motions during the peak of the flare were *along* the flare ribbons. This is inconsistent with the 'spreading ribbons' pattern expected from an evolving 2-dimensional flare arcade. The coronal electric field calculated from these motions appeared to correlate with HXR flux at the time of the major HXR peak, but the correlation was poor at other times in the flare. This, the authors suggested, may mean (a) that the reconnection geometry is generally not describable as a quasi-2-dimensional structure, (b) that the early phase of the flare does not involve systematic motion, or (c) that particle acceleration is only directly determined by the coronal electric field during a short part of the flare.

Measurements of the reconnecting flux, or electric field during large two-ribbon events have been attempted by Poletto and Kopp (1986), Fletcher and Hudson (2001), Saba, Gaeng, and Tarbell (2001) and Qiu *et al.* (2002). Field strengths range from a few to the order of 100 V cm^{-1}, with these being generally highest at the impulsive peak.

One further relevant piece of work is the study of HXR ribbons using *Yohkoh* HXT during the peak of the 14 July 2000 flare (Masuda, Kosugi, and Hudson, 2001). In this rare observation with HXT, a number of discrete HXR sources were observed to brighten at locations along the flare ribbons. By assuming that at any instant in time the brightest kernels were linked in that they mapped the ends of

TABLE I
Event list (times in UT).

Date	Start	Peak	End	Class	Region
14 March 2002	01:38	01:50	02:02	M5.7	9866
17 March 2002	19:24	19:31	19:34	M4.0	9871
10 April 2002	12:23	12:31	12:40	M8.2	9893
17 July 2002	06:58	07:13	07:19	M8.5	0030

just-reconnected field, the authors suggested that HXR kernel motions were consistent with the reconnection of progressively less and less sheared field, and that the HXR spectrum resulting from the earlier reconnection (more sheared) is harder than that occurring later on.

In Section 2 we will describe selection of data used in our study. Section 3 presents the time variation of hard X-ray spectra throughout the events studied, and Section 4 the imaging of footpoints in the flare impulsive phase. We focus on more detail on one of our events in Section 5 and discussion and conclusions are presented in Sections 6 and 7.

2. Data Selection

We selected a number of RHESSI flares, initially on the basis of their GOES classification. We wanted to make images at a time resolution on the order of the spin period of the spacecraft (~ 4 s), in the 30–50 keV spectral range (which should be unambiguously non-thermal emission). Typically, a good back-projected image will require ≥ 2000 counts totaled over all grids being used, corresponding to on the order of 500 counts s^{-1}. Flares of GOES class M4 and above tend to have a count rate in the 30–50 keV range sufficient to make 20+ images over the duration of the impulsive phase, from which we can hope to see some systematic motion. Further, we required that the reconstructions must have two footpoints visible throughout the peak – this is not always the case. Sometimes one footpoint disappears into the level of the noise. Or if events are too near the limb, projection effects can make it difficult or impossible to separate footpoints. A further selection based on preliminary reconstructions, and flare positions, results in a short list of events studied, given in Table I.

3. Hard X-Ray Spectra

At the time of writing the RHESSI data have only preliminary calibrations, even though the energy resolution is essentially at the design level in eight of the nine Ge detectors, and all are aligned precisely in gain. We have therefore restricted our analysis of the spectra to broad energy bands and to relative variations within each flare, omitting detector G2 (Lin *et al.*, 2002). We do not attempt full imaging spectroscopy, but instead work with these broad-band counting rates independently for imaging and spectroscopy. We accumulate counts in two-second bins, which approximately cancels out any modulations resulting from the spacecraft spin, which is held to the range 14–15 rpm. Residual modulations result in a roughly random fluctuation excess over the photon-counting noise statistics.

Previous observations with Ge resolution have shown that the hard X-ray spectrum does not follow an exact power-law distribution, but may show a rather sharp spectral break between two power laws (Lin and Schwartz, 1987). Spectra obtained at lower energy resolution (Elcan, 1978) suggest that this property may be fairly general, and that the break energy commonly occurs at about 50 keV. In addition to this spectral feature, we know that the soft X-ray spectrum closely matches that expected from a Maxwellian particle distribution, i.e., an exponential bremsstrahlung continuum in the hard X-ray range. The effective temperature of this distribution increases with the photon energy observed, suggesting a multi-thermal plasma (Lin and Schwartz, 1987). The detailed properties of the hard X-ray spectra remain to be delineated by RHESSI data, but the existing data often fit an essentially six-parameter spectral distribution in the 10–100 keV range: temperature and emission measure for a hot or 'super-hot' thermal plasma, with temperature typically not exceeding about 40 MK (3.4 keV); plus the parameters of the broken power law at higher energies.

The first question regards the reality of the soft–hard–soft behavior as seen with RHESSI's greater spectral purity. We define three broad energy bands, with edges at 20, 30, 50, and 70 keV, and plot time profiles of flux (30–50 keV) and the two hardness ratios in Figure 1. Broad energy bands are necessary for good signal-to-noise ratio, and we use the two bands to determine if the same pattern persists both above and below the typical break energy of the double power law. For all four events studied, the soft–hard–soft pattern, and the correlation between flux and spectral hardness is clearly visible in both ratios over bursts down to time scales of ~ 10 s.

With broad-band hard X-ray observations there is the clear possibility that the soft–hard–soft pattern might be confused in any two-band comparison, if either band contained appreciable thermal counts. Although the thermal component is expected to be negligible above 20 keV, we test for its presence using flux-flux correlation plots. At low energies (10–20 keV) a flux-flux correlation plot tends to show loops resulting from the slower growth of thermal emission (Figure 2). At higher energies, such as the 30–50 keV band used in Figure 1, the correlation

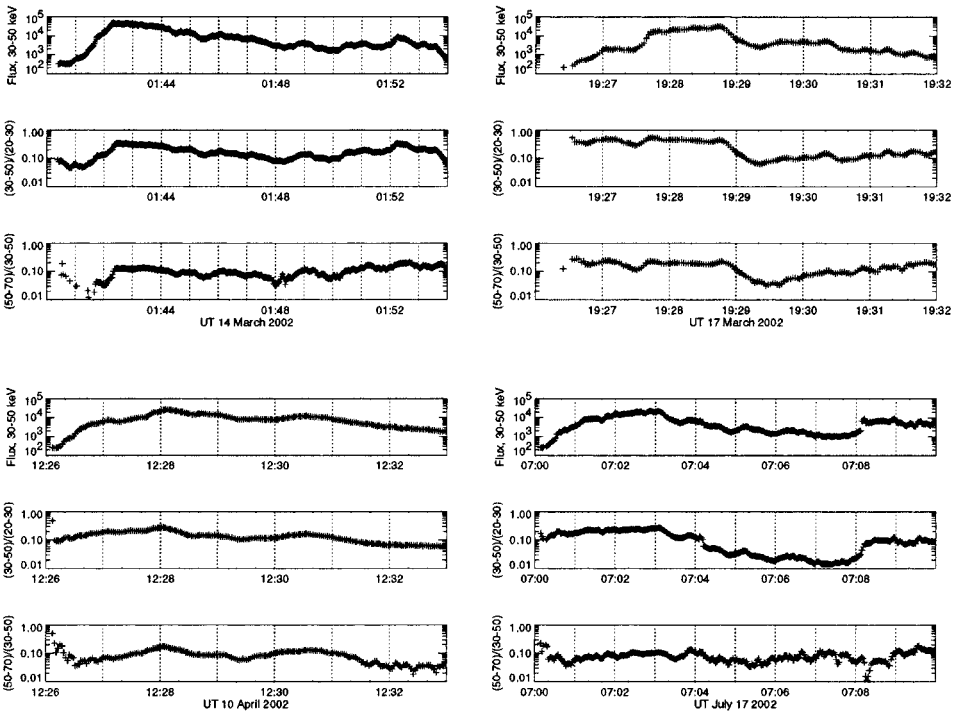

Figure 1. Broad-band light curves at 30–50 keV (*upper plots*) and two representative spectral ratios for the four events listed in Table I. The ratios are for adjacent broad bands with edges at 20, 30, 50, and 70 keV. Note the systematic tendency for these hardness ratios to correlate directly with the flux. *Dotted lines* show minutes.

tends to be direct. Because this also rules out appreciable energy-dependent trapping (e.g., Aschwanden *et al.*, 1999), we confirm that the soft–hard–soft pattern originates in the acceleration mechanism itself.

A further test (not shown) of the contribution of thermal sources in our broad RHESSI bands is made by taking advantage of the high spectral resolution of the RHESSI detectors, and correlating 1-keV energy bands against the broad bands defined for Figures 1 and 2. The correlations show that the gradual component is restricted mainly to the energy range below 20 keV, and that each of the correlation coefficients peaks close to the center of the relevant energy band. Thus we are confident that 'contamination' across the edges of the chosen bands is minimal.

4. Imaging of Impulsive Phase Footpoints

In each of the events, we have divided up the flare impulsive phase into a number of time bins, which are integer multiples of half of the spacecraft spin period. The criterion for selecting the bin size was simply to get sufficient counts in the bins at the beginning and end of the event; in practice this corresponds to a S/N

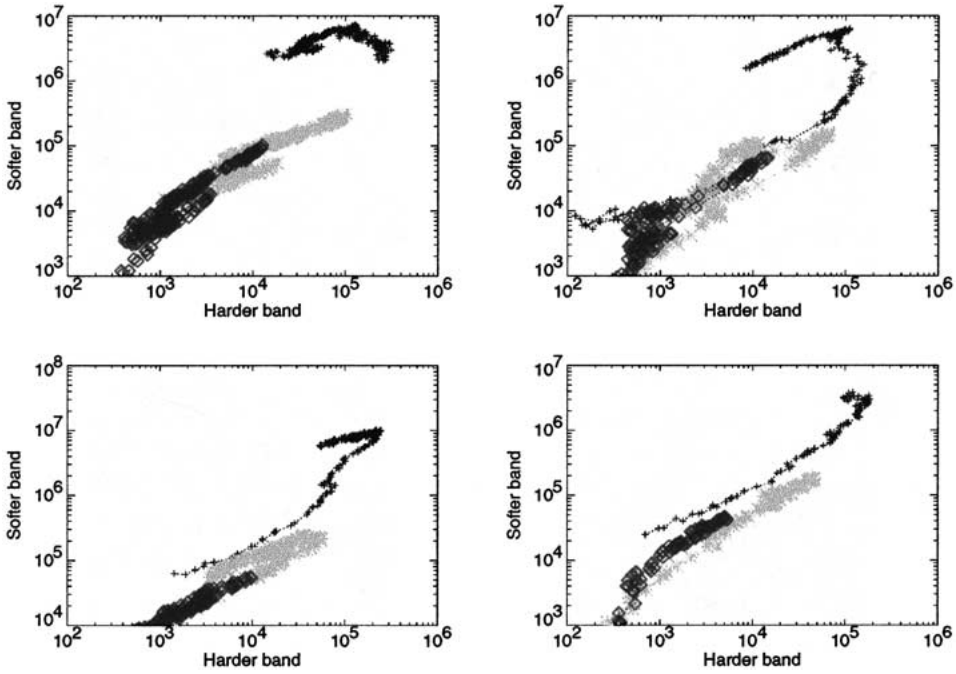

Figure 2. Pairwise correlation plots of broad-band flux ratios for the four flares studied, with the harder and softer bands set with boundaries at 10, 20, 30, 50, and 70 keV. The 'hysteresis' loops at the lowest energies (*pluses*) show the presence of an uncorrelated slowly-varying component, identified with the hot flare plasma or the 'super-hot' component reported by Lin and Schwartz (1987). At the highest energies (*diamonds*) the correlation is almost the same for burst rise and fall (see CD-ROM enclosure).

ratio between source (following CLEAN processing, see below) and background of S/N ≥ 3. This means that in general there are unequal numbers of counts in each bin, and a variable S/N ratio on the reconstructed images. However, we felt that it was important that all components on the (u, v)-plane be equally sampled. We have used all grids down to and including grid 3, which has a FWHM of 6.8 arc sec. This provides adequate resolution for centroiding, and is reasonably quick to run for a large number of images. Following back-projection using the standard RHESSI software, the images were further processed using the CLEAN algorithm (e.g., Christiansen and Högbom, 1969), also implemented as part of the RHESSI software. The CLEAN technique assumes that the source distribution can be represented as a number of point sources, and can therefore be poor at imaging large diffuse sources. However, we have good reason to expect the 30–50 keV impulsive-phase chromospheric emission to be well-approximated by a set of point sources.

The footpoints were identified by summing the CLEANed images. Frequently, more than two footpoints are visible; in such cases it is extremely useful to also have TRACE imaging data or MDI magnetograms available to identify all foot-

points occurring on the same side of the magnetic neutral line, and hence identify the most likely conjugate pairs. A selection box is drawn around all footpoints on one side of the magnetic neutral line, and the (intensity-weighted) centroid of this box located within each time frame. A continuous motion of a single bright source of emission would thus show up as a continuous line of centroid positions, whereas if sources were brightening and dimming in succession but not moving, a cluster of centroids would be found at each location. These are two extremes of what is generally a rather complex pattern of footpoint brightenings; in reality each flare requires rather detailed study to interpret what is going on. However, in this first paper we are searching only for gross patterns.

Figure 3 shows maps of footpoint centroid location for the flares listed in Table I. These generally reveal a fairly systematic variation in footpoint position as a function of time, often *along* ribbon-like patterns, though the scatter can be considerable. A measure of the rate at which the footpoints separate is given by plotting the distance between conjugate pairs of centroids as a function of time. Figure 4 (lower panels) shows the variation of footpoint separation with time, and the 30−50 keV flux over the same interval.

There are variations in the footpoint separations well above the level of the fluctuations on the centroided positions. Table II shows average separation speeds during the intervals of most rapid change. The fluxes and ratios at the times of these sudden motions are mostly increasing (i.e., the spectrum is hardening) regardless of whether there is a positive or negative footpoint velocity. In the cases of 14 March 2002 and 17 March 2002 a sudden motion matches well with the peak flux (maximum hardness). However, at this time resolution, in general there is no clear correlation between times of peak flux and high separation rates.

We have also looked at times of minimal change in footpoint separation in the four flares, as summarized in Table III. There is a tendency for a dip or decrease in the flux ratios during these times, however, the fluxes themselves may be high (spectra hard) or low (spectra soft).

5. The 14th March 2002 Event

In this section we focus on the event of 14 March 2002. If we plot, instead of the centroids of the CLEAN boxes, the locations of the CLEAN sources themselves (i.e., ignoring the contribution of the residuals) we find that the HXR kernels in the early part of the flare are spread out, suggesting systematic motions along a ribbon (Figure 5) that might have been underestimated in Figure 4. Centroiding on the data *including* the residuals, as we do in Section 4, tends to weight the source position towards the center of the centroiding box, so that variations (both systematic, and noise) in source position are generally reduced. The residuals contain information about the side-lobes which should not be discarded, which is why we have chosen in general to centroid on the CLEAN maps in Section 4. However we find, for

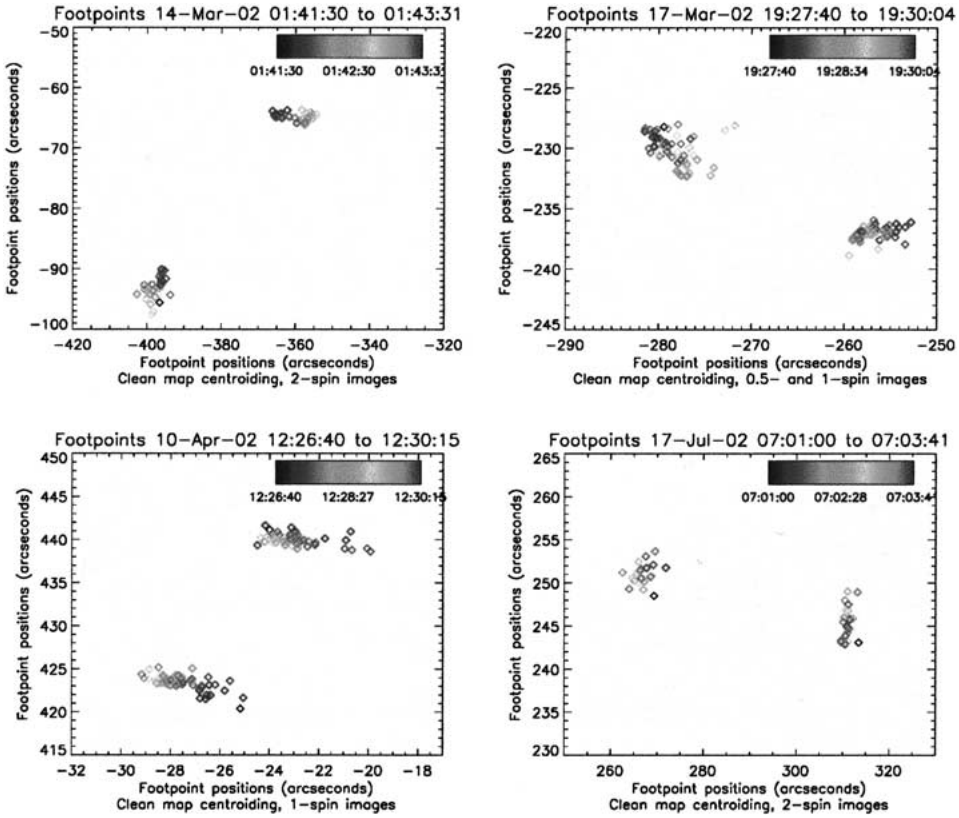

Figure 3. Footpoint locations derived from the CLEAN maps, color-coded by time in the original (see CD-ROM enclosure).

TABLE II

Mean speeds during periods of rapid variation in footpoint separation.

Date	Time (UT)	Average separation rate (km s^{-1})	Flux ratios/ fluxes
14 March 2002	01:42:20–01:42:40	$+390 \pm 30$	increasing
	01:43:15–01:43:30	-370 ± 30	increasing
17 March 2002	19:28:30–19:28:45	-480 ± 80	increasing
	19:28:45–19:29:00	$+360 \pm 60$	decreasing
	19:29:00–19:29:15	-360 ± 60	decreasing
10 April 2002	12:27:00–12:27:30	-90 ± 15	increasing
	12:27:30–12:27:50	$+95 \pm 15$	increasing
17 July 2002	07:01:20–07:02:30	$+55 \pm 5$	increasing

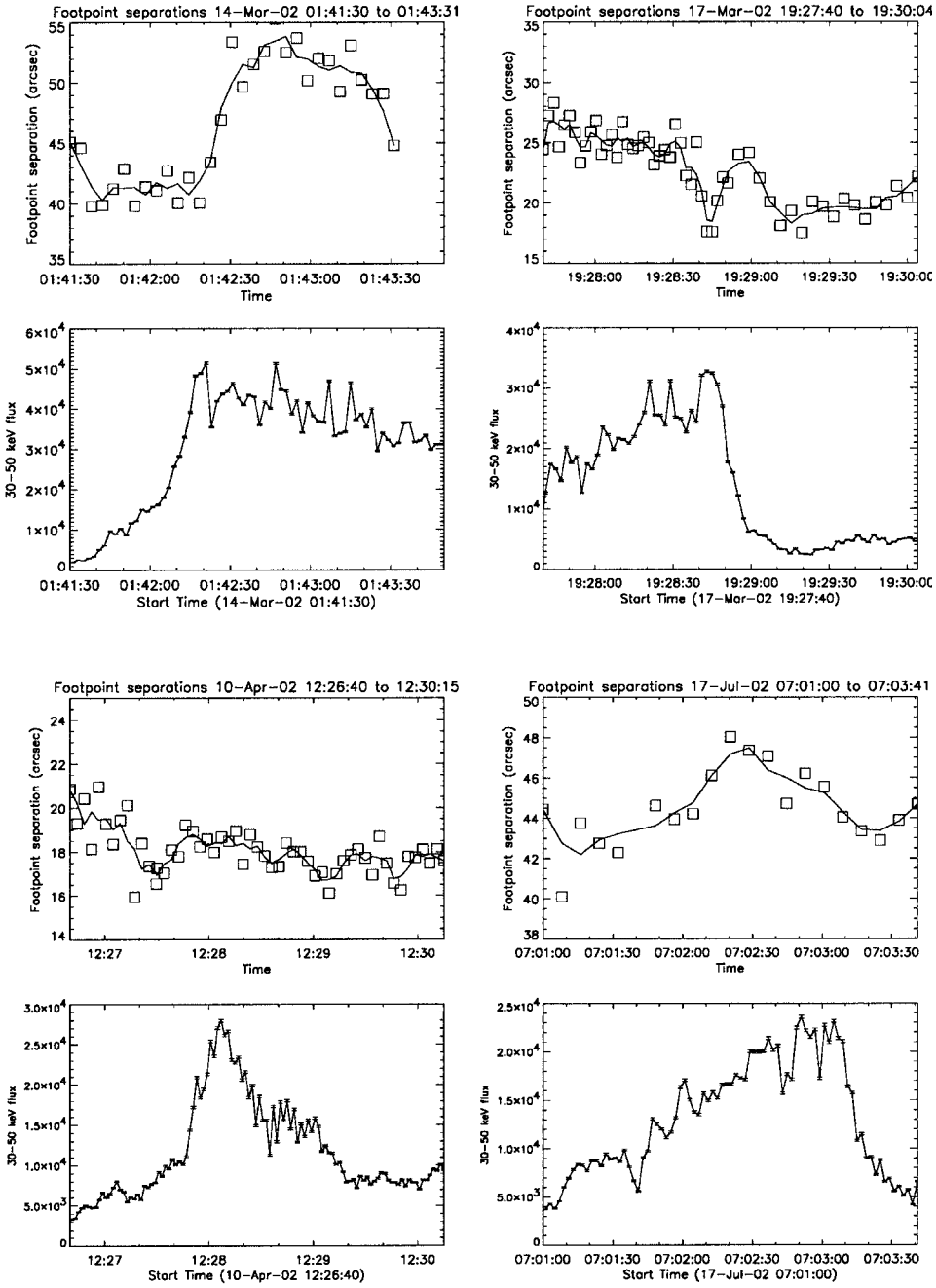

Figure 4. Apparent separation of footpoint sources, and the corresponding 30–50 keV flux. A 3-point running mean is drawn through the source positions. In the 14 March 2002 flare the separation varies smoothly, with an r.m.s. fluctuation around its smooth trajectory on the order of one arc sec. In the 17 March 2002 event the variation is not so systematic, but changes well above the level of the centroiding noise are clear. The 10 April 2002 event shows strong fluctuations in footpoint separation, and the 17 July 2002 shows a fairly systematic increase and decrease of separation throughout the impulsive phase. (All times in UT.)

TABLE III
Steady separation intervals.

Date	Time (UT)	Flux ratios
14 March 2002	01:41:30–01:42:20	ratios dip
	01:42:30–01:43:40	decreasing slightly
17 March 2002	19:27:50–19:28:30	decreasing
	19:29:20–19:30:00	ratios dip
10 April 2002	12:27:50–12:28:30	peak then decrease

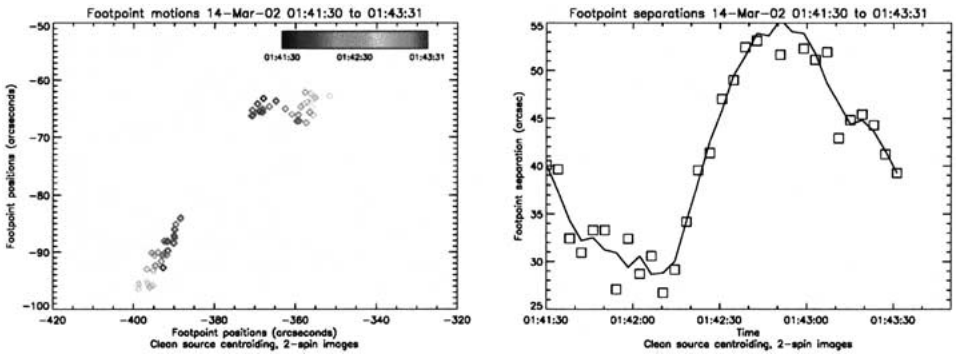

Figure 5. Left: CLEAN source centroids (as opposed to CLEAN map centroids) during the 14 March 2002 flare, showing systematic motion along a ribbon. *Right:* the footpoint separations derived from the CLEAN sources (see CD-ROM enclosure). (Times in UT.)

the evolution of the 14 March 2002 event, that the CLEAN sources alone contain valuable position information. This event was well-covered by Transition Region and Coronal Explorer (TRACE) observations in the 171 Å band (Handy *et al.*, 1999) primarily imaging plasma emitting in the Fe IX/X complex. Using these images allows us to form a better idea of the geometry of this event, and confirms the ribbon interpretation.

The TRACE images were de-spiked and corrected for the known offset between the pointing information (from the white-light channel) and the true pointing of the EUV channel. The cadence of the TRACE images is 12 s, and at this cadence the flare shows rapid evolution in the EUV, with a number of bright sources appearing to move along two ribbons, suggestive of initial rapid changes in the core of a highly sheared arcade. Post-flare images confirm bright, still sheared, loops joining these ribbons. A further correction, due to systematic TRACE pointing drifts as the telescope flexes thermally through its orbital motion, is needed to align the brightest TRACE and RHESSI sources; this is done by eye but the same offset of [−6 arc sec, 12 arc sec] is adequate to give good correspondence through all of the impulsive phase. Figure 6 shows the flare ribbons and footpoints through the

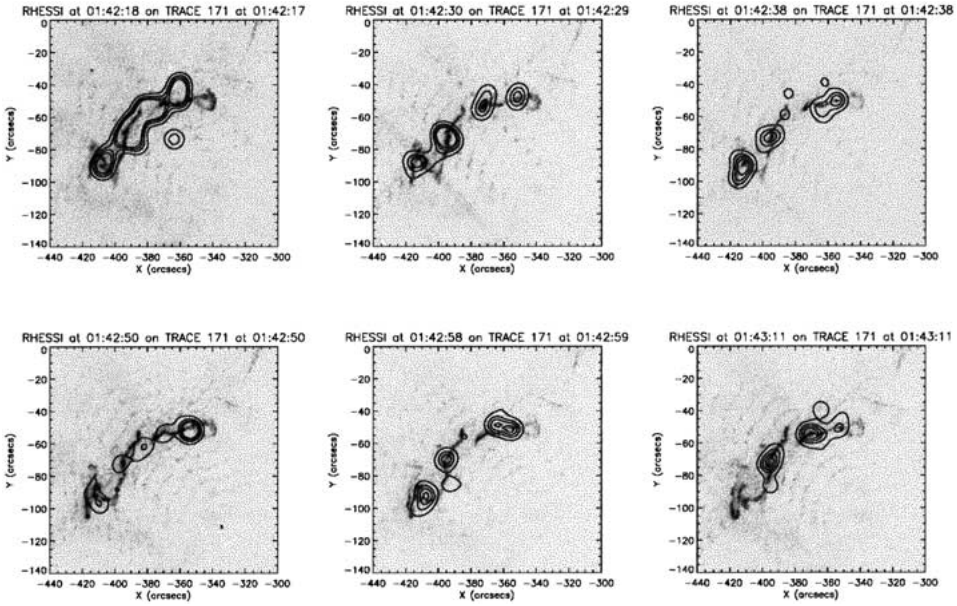

Figure 6. The impulsive peak of the flare of 14 March 2002. RHESSI contours, at 25%, 50%, 70%, and 90% of the maximum in each frame are overlaid on the nearest TRACE image. At the relatively low spatial resolution afforded by grid 3, there is a good correspondence between HXR sources and the brightest 171 Å flare kernels. The coordinates shown here are those given by the TRACE pointing, which, during this event, is offset from that of RHESSI by (+6 arc sec, −12 arc sec). (Times in UT.)

peak of the impulsive phase. The brightest HXR sources tend to align well with the brightest TRACE 171 Å sources. This has been noted previously by Fletcher and Hudson (2001).

Following these rapid changes at the beginning of the flare, the field settles down to a slower evolution, with HXRs emitted by two main sources (the two strongest RHESSI sources visible in the bottom right panel of Figure 6). We have made reconstructions in the 20–30 keV energy band throughout the first 12 min of this flare. There were inadequate counts in the 30–50 keV band to use this for the whole interval. Following our analysis of the contribution of thermal or gradual phase fluxes to the various energy bands, we can be certain that the majority of 20–30 keV emission is non-thermal and thus reflects footpoint locations. The footpoint separation rate as a function of time is shown in Figure 7. We see that following the main impulsive peak there is a drop in the separation, as the source at (−395 arc sec, −70 arc sec; see caption for Figure 6) becomes dominant, then a slow rise over the next five minutes or so, as these two strong footpoints separate. Fitting a smooth line between 01:45 and 01:50 UT, we find an approximately linear separation increase of about 8.9 km s^{-1}, suggesting a phase of slow reconnection. After an impulsive phase which was rather complicated, the gradual phase field evolution appears much simpler.

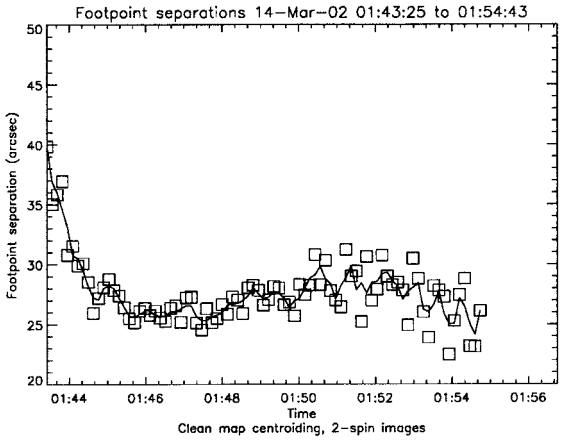

Figure 7. The footpoint separation in the 14 March 2002 event as measured in the 20–30 keV band, for the remainder of the full event. For the interval 01:45–01:50 UT the separation increases almost linearly at an apparent speed of 8.9 km s^{-1} with a residual scatter of 0.7 arc sec, a measure of the RHESSI centroiding precision for 8-s integrations in a flare of this brightness.

6. Discussion

In the extraction of coronal magnetic energy, the magnetic mapping between the energy source and the footpoint brightenings should lead to correlations between the rate of dissipation of stored coronal energy and the footpoint motions. We have investigated one possible correlation: that between the spectral hardness (defined by the ratio of two broad energy bands) and the centroided footpoint motion.

Our small number of events makes it impossible to draw any general conclusions about the time behavior of flare footpoints, but we have noted the following patterns with some frequency: (1) systematic HXR footpoint motions along flare ribbons; (2) the occurrence of cases of approach of footpoints, and (3) episodes of rapid change followed by relative stability. The first of these is consistent with what has been seen previously by Qiu *et al.* (2002) in Hα, and the separation–time curves for these events do show a smooth evolution in time, suggestive of evolution through an arcade structure, albeit a highly sheared one. However, it is clear in some cases that the impulsive-phase evolution is not particularly smooth, and may result from the lighting-up of different flux elements in a patchy way as time proceeds, rather than a smooth evolution through a continuous field. We find an overall tendency for episodes of rapid footpoint motion to correspond to times when the flux ratio is increasing, whereas when the footpoint separation is not varying much the flux often decreases or goes through a dip. However, a pattern of high flux occurring with rapid footpoint motion is not readily visible.

The event of 14 March 2002 (and to a lesser extent 17 March 2002) is an example which suggests a link between flare energy production and apparent footpoint motions, as expected from the magnetic nature of a flare (Priest and Forbes,

2002). Figure 3 shows a sudden increase of footpoint separation in the time range 01:42:20–01:42:40 UT, just the time of maximum HXR luminosity (see Figure 1 and Table II). The rapid separation speed during this interval is approximately 390 km/s, but as can be seen in Figures 3 and 5 the motion may be a combination of a continuous motion of one footpoint, and a discrete sideways 'jump' in the location of the other. However, until more precise theoretical work can be done (see Section 1), and until we include the measured magnetic field strength in our calculations, we cannot be sure that the observed speed has even the right order of magnitude to explain the energy release in the context of the coronal magnetic field at the time of the flare. It is worth noting that a speed of this magnitude exceeds the Alfvén or sound speeds below the transition region, the assumed footpoint height, and would thus have to be the result of a coronal process.

7. Conclusions

RHESSI confirms, with high spectral and temporal resolution, the soft–hard–soft pattern in solar flares. This paper has focused on an effort to relate this spectral pattern to the flare geometry, and at the same time to explore the RHESSI capability for such studies. We find that the RHESSI data can be used to delineate footpoint motions in flares as small as a higher M class on time scales of a few seconds, and with a precision on the order of 1 arc sec (r.m.s.) even omitting data from the two finest collimators. The observations show systematic patterns of apparent footpoint motion, but these vary from flare to flare and do not resemble the simple increase of footpoint separation expected from 2D reconnection models and from Hα ribbon behavior. The observations suggest a pattern of behavior in which the initial hardening of the spectrum is accompanied by rapid source movements or new sources appearing, whereas during episodes of negligible change in source position, the spectrum softens again. This is consistent with the spectral hardness being linked to the instantaneous conditions in the reconnection region. Further studies, particularly on larger X-class flares, combined with magnetic field reconstructions, may be able to open this link to study; for example, is there a direct correlation with global magnetic conditions in a reconnecting current sheet, as described for example by Litvinenko (1996)? Or a less direct correlation might suggest that the micro-physical conditions – turbulence level, temperature, etc. are important as would be the case for a stochastic accelerator. Benz (1977) has shown that the soft–hard–soft pattern is consistent with a stochastic acceleration process, and geometrical studies based on hard X-ray energy release may be able to locate the regions where this happens. Following the discussion in the Introduction, we would expect these regions to correspond to the sources of energy made available for particle acceleration by the coronal restructuring.

The soft–hard–soft spectral pattern dominates the bursty impulsive phase of a flare, but some events show a soft–hard–harder pattern (e.g., Frost and Den-

nis, 1971) on longer time scales; this may be correlated with geo-effectiveness (Kiplinger, 1995). We would therefore like to extend the present study, taking advantage of RHESSI's capability for imaging spectroscopy to relate spectral and spatial morphologies, to study this different kind of behavior as well.

Acknowledgements

NASA supported this work via NAS 5-9833 at UC Berkeley (HSH). L.F. would like to acknowledge travel support from the Nuffield Foundation and from PPARC. We thank many RHESSI team members, especially S. Krucker on image technique, for help of various kinds.

References

Aschwanden, M. J. Fletcher, L., Sakao, T., Kosugi, T., and Hudson, H.: 1999, *Astrophys. J.* **517**, 977.
Benz, A. O.: 1977, *Astrophys. J.* **211**, 270.
Christiansen, W. N. and Högbom, J. A.: 1969, *Radiotelescopes*, Cambridge, University Press, Cambridge.
Dennis, B. R.: 1985, *Solar Phys.* **100**, 465.
Elcan, M. J.: 1978, *Astrophys. J.* **226**, L99.
Fletcher, L. and Hudson, H.: 2001, *Solar Phys.* **204**, 69.
Handy, B. N. *et al.*: 1987, *Solar Phys.* **187**, 229.
Kiplinger, A. L.: 1995, *Astrophys. J.* **453**, 973.
Kosugi, T., Masuda, S., Makishima, K., Inda, M., Murakami, T., Dotani, T., Ogawara, Y., Sakao, T., Kai, K., and Nakajima, H.: 1991, *Solar Phys.* **136**, 17.
Lin, R. P. and Schwartz, R. A.: 1987, *Astrophys. J.* **312**, 462.
Lin, R. P. *et al.*: 2002, *Solar Phys.*, this issue.
Litvinenko, Y. E.: 1996, *Astrophys. J.* **462**, 997.
Masuda, S., Kosugi, T., and Hudson, H. S.: 2001, *Solar Phys.* **204**, 55.
Parks, G. K. and Winckler, J. R.: 1969, *Astrophys. J.* **155**, L117.
Poletto, G. and Kopp, R. A.: 1986, in D. F. Neidig (ed.), *The Lower Atmosphere of Solar Flares; Proceedings of the Solar Maximum Mission Symposium*, Sunspot, New Mexico, National Solar Observatory, p. 453.
Priest, E. R. and Forbes, T. G.: 2002, *Astron. Astrophys. Rev.* **10**, 313.
Qiu, J., Lee, J., Gary, D. E., and Wang, H.: 2002, *Astrophys. J.* **565**, 1335.
Saba, J. L. R., Gaeng, T., and Tarbell, T. D.: 2001, in P. C. H. Martens and D. Caufman (ed.), *Multi-Wavelength Observations of Coronal Structure and Dynamics – Yohkoh 10th Anniversary Meeting*, Kailua-Kona, Hawaii, Elsevier Science, p. 96S.
Sakao, T., Kosugi, T., and Masuda, S.: 1998, in T. Watanabe, T. Kosugi, and A. C. Sterling (ed.), *ASSL Vol. 229: Observational Plasma Astrophysics: Five Years of YOHKOH and Beyond*, Tokyo, p. 273.